Available at www.sciencedirect.com

ScienceDirect

journal homepage: www.elsevier.com/locate/he

Evolution of an [FeFe] hydrogenase with decreased oxygen sensitivity

Alyssa S. Bingham [a,1], Phillip R. Smith [a,2], James R. Swartz [a,b,*]

[a] Department of Chemical Engineering, Stanford University, 381 North South Mall, Stauffer III, Room 113, Stanford, CA 94305-5025, USA
[b] Department of Bioengineering, Stanford University, 381 North South Mall, Stauffer III, Room 113, Stanford, CA 94305-5025, USA

ARTICLE INFO

Article history:
Received 25 November 2010
Received in revised form
1 February 2011
Accepted 8 February 2011
Available online 22 March 2011

Keywords:
Hydrogenase
Oxygen tolerance
Protein engineering
Directed evolution

ABSTRACT

[FeFe] hydrogenases catalyze the rapid combination of protons and electrons into hydrogen, but their oxygen sensitivity limits their use in clean renewable hydrogen production applications. The catalytic activity of current [FeFe] hydrogenases is destroyed by oxygen. Here, the discovery of mutant [FeFe] hydrogenases with decreased oxygen sensitivity is described. The new hydrogenases are derived from [FeFe] hydrogenase I of *Clostridium pasteurianum* (CpI). A cell-free protein synthesis-based screening platform was used to identify an initial mutant from a randomly mutated CpI library. Three mutations were cooperatively responsible for the decreased oxygen sensitivity, and further improvements were identified by saturation mutagenesis at the influential sites. After oxygen exposure under conditions where the enzyme is in the resting state, the mutant hydrogenase retains significantly higher methyl viologen reduction activity than the wild-type enzyme. However, surprisingly, when the enzyme is actively catalyzing hydrogen production during oxygen exposure, the mutant hydrogenase shows no improved oxygen tolerance. This observation highlights the complexity of the oxygen inactivation process in CpI and demonstrates the need to develop a screen that measures hydrogenase oxygen tolerance during catalysis.

1. Introduction

[FeFe] hydrogenases catalyze the rapid, reversible combination of protons and electrons into hydrogen gas, H_2. Ideally the hydrogen production capability of these catalysts could be harnessed for clean renewable hydrogen production as a fuel source and chemical feedstock [1,2]. One possible application is direct biohydrogen production, in which an engineered photosynthetic organism would split water to produce protons and electrons and a non-native hydrogenase would convert these into hydrogen gas, which could then be harvested. The major limitation to these applications, however, is the oxygen sensitivity of the hydrogenase [3]. Even low partial pressures of oxygen, either produced by photosynthesis or present in the atmosphere, are likely to destroy the catalytic activity of current [FeFe] hydrogenases [4].

There are three main classes of hydrogenases: the [FeFe] hydrogenase, the [NiFe] hydrogenase, and the [Fe]-only hydrogenase [5], named for the metals at the active site of the enzyme. The [FeFe] hydrogenase is especially interesting for biotech applications because of its fast rate of H_2 production [3,6]. The [FeFe] hydrogenase active site consists of a [2Fe]

* *Corresponding author*. Department of Chemical Engineering, Stanford University, 381 North South Mall, Stauffer III, Room 113, Stanford, CA 94305-5025, USA. Tel.: +1 650 723 5398; fax: +1 650 725 0555.
E-mail addresses: abingham@stanford.edu (A.S. Bingham), psmith2@stanford.edu (P.R. Smith), jswartz@stanford.edu (J.R. Swartz).
[1] Tel.: +1 650 723 0274; fax: +1 650 725 0555.
[2] Tel.: +1 650 724 4969; fax: +1 650 725 0555.
0360-3199/$ – see front matter
doi:10.1016/j.ijhydene.2011.02.048

subcluster activated by 3 carbon monoxide and 2 cyanide ligands and a dithiol bridge. A bridging cysteinyl sulfur connects this [2Fe] cluster to a [4Fe4S] cluster to form the complete H-cluster [7]. In some [FeFe] hydrogenases, such as *Clostridium pasteurianum* hydrogenase I (CpI), three accessory [4Fe4S] clusters and a [2Fe2S] cluster are believed to transfer electrons between the electron donor or acceptor at the protein surface and the active site at the center of the protein [8,9].

Stripp et al. have proposed an oxygen inactivation mechanism for [FeFe] hydrogenases; oxygen is believed to first bind to the distal Fe of the $[2Fe]_H$ subcluster, then form a reactive oxygen species that destroys the $[4Fe4S]_H$ subcluster [10]. The distal Fe, the Fe farthest from the $[4Fe4S]_H$ cluster, is believed to be the hydrogen binding site and also the site of reversible carbon monoxide binding and inhibition [11,12]. Oxygen inactivation has been studied using protein film electrochemistry, where the hydrogenase is adsorbed to an electrode and its activity directly measured by electron transfer through the electrode under oxidizing or reducing potentials during oxygen exposure [13–15]. Protein film electrochemistry experiments have demonstrated that reversible carbon monoxide inhibition protects against oxygen inactivation, supporting the proposed mechanism of O_2 binding at the distal Fe atom [10].

Protein film electrochemistry experiments have also been used to develop a simplified model of [FeFe] hydrogenase oxygen inactivation. Goldet et al. have proposed that two steps may be rate limiting in oxygen inhibition: (1) the diffusion of oxygen through the protein to the active site pocket, and (2) the binding of oxygen to the $[2Fe]_H$ subcluster [16]. Both this model and the mechanism proposed by Stripp et al. only describe the oxygen sensitivity in terms of the active site. The role accessory [FeS] clusters may play in the oxygen inactivation mechanism, and the oxygen sensitivity of the accessory [FeS] clusters themselves [17], are not considered.

The accessory [FeS] clusters in some [NiFe] hydrogenases, however, appear to influence oxygen tolerance. [NiFe] hydrogenases are reversibly inactivated by oxygen [12]. Upon oxygen exposure they enter one of two states, characterized by slow (Ni-A) or rapid (Ni-B) reactivation after removal of oxygen [18]. Several oxygen-tolerant [NiFe] hydrogenases have been identified [19–21], and while none appear to enter the Ni_u-A state, multiple different mechanisms appear responsible for imparting oxygen tolerance [22]. In the membrane-bound hydrogenase of *Ralstonia eutropha*, the high redox potential of the proximal accessory [4Fe4S] cluster appears to protect the active site from the inactivated state [22,23]. In contrast, the oxygen resistance of the regulatory hydrogenase of the same organism is dependent on bulky amino acids blocking the hydrophobic channels to the active site [24]. In this enzyme, mutating these amino acids to smaller residues makes the hydrogenase sensitive to oxygen inactivation [24]. While some [NiFe] hydrogenases have the advantage of oxygen tolerance, these enzymes typically work in the hydrogen consumption direction and are relatively slow hydrogen producers compared to [FeFe] hydrogenases [3,5,6].

One approach proposed for the improvement of oxygen tolerance of [FeFe] hydrogenases is to limit diffusion of oxygen molecules to the active site [25]. Based upon this hypothesis, a screen developed by Boyer et al. [26] and by Stapleton and Swartz [27] was chosen to screen for mutant hydrogenases that would retain more activity after oxygen exposure than the wild-type protein. In this screen, mutated hydrogenases were first expressed and activated in cell-free protein synthesis reactions. The hydrogenase activities were then measured before and after oxygen exposure. It was believed that if the protein structure could be modified to better exclude oxygen, the active site would be protected whether or not the enzyme was actively catalyzing the hydrogen conversion reaction at the time of oxygen exposure. For convenience, the exposure was performed by adding air-saturated buffer in the absence of catalytic substrates. It was further believed that improved enzymes would be detected by measuring the remaining activity in either the hydrogen production or hydrogen consumption direction. Because the reactions were conducted in an anaerobic 2% hydrogen environment, the activity before and after exposure was measured in the hydrogen consumption direction using methyl viologen reduction as the indicator of activity.

Here, the identification of mutated CpI hydrogenases that are significantly more stable against oxygen inactivation is described. These mutants, unexpectedly, do not show improved oxygen tolerance when exposed while actively performing catalysis. The oxygen sensitivity of the protein is here defined as the extent to which the enzyme loses methyl viologen reduction activity after oxygen exposure.

2. Materials and methods

2.1. Plasmids

For cell-free expression of [FeFe] hydrogenase I from *C. pasteurianum* (CpI) for the library screen, the pK7sCpI plasmid [26] containing the gene *hydA* from *C. pasteurianum* was used. The gene was codon optimized for expression in *Escherichia coli*, and the first 15 bases were optimized to minimize mRNA secondary structure. For subsequent cell-free expression of mutants created by site-directed mutagenesis or saturation mutagenesis, either the pK7sCpI or the pET-21(b)CpI plasmid [28] was used.

For *in vivo* protein production, the plasmid pET-21(b)CpI was used to express CpI with a C-terminal *Strep*-tag II sequence (IBA GmbH, Germany) [28]. The plasmid pACYCDuet-1-*hydGX-hydEF* was used for co-expression of the three maturation proteins from *Shewanella oneidensis* responsible for activating the hydrogenase [28].

2.2. Mutagenesis and library creation

The cell-free protein synthesis-based screening platform for [FeFe] hydrogenases developed by Boyer et al. [26] and Stapleton and Swartz [27] was modified to create and screen a library of mutant CpI hydrogenases for decreased oxygen sensitivity. Specifically, for this mutant library, random mutagenesis was performed using error-prone PCR with the nucleotide analogs dPTP and 8-oxo-dGTP [29]. The concentration of nucleotide analogs was varied between 2 μM and 200 μM, and the number of cycles for the first PCR reaction was varied between 20 and 30 cycles. For the final library, the PCR reaction contained 8 μM each of dPTP and 8-oxo-dGTP (TriLink

BioTechnologies, Inc., San Diego, CA), 0.2 mM dNTPs, 0.5 μM forward and reverse primers, 1X Taq PCR buffer, 1.5 mM $MgCl_2$, 0.05 U/μL Platinum Taq polymerase, and 1 ng of the pK7sCpI plasmid. The forward and reverse primers were designed to bind upstream of the T7 promoter and ribosome binding site and downstream from the T7 terminator, respectively, and both were designed with a 5′ homoprimer K4 extension (TCAGACTGGACACTAAATGG) [30]. The PCR reaction was conducted with an initial incubation at 95 °C for 3 min, followed by 25 cycles of 95 °C for 45 s, 55 °C for 45 s, and 72 °C for 4 min, and then completed by incubating at 72 °C for 10 min. The PCR product was purified using the QuiQuick PCR cleanup kit (Qiagen, Valencia, CA).

The PCR product from the first reaction was then used as a template for a second round of PCR, where the same PCR reaction protocol and cleanup kit were used in the absence of the nucleotide analogs to create the final mutant library. This DNA library was then diluted and amplified using single-molecule PCR [31] with the homoprimer K4 [30] as previously described by Stapleton and Swartz [27]. This was performed in 96-well or 384-well plates where most wells contained the amplified PCR product for a single CpI mutant.

2.3. Cell-free protein synthesis of CpI

This collection of amplified CpI mutant genes was then transferred to an anaerobic glove box (Coy Laboratories, Grass Lake, MI) and used as the DNA template for cell-free protein synthesis [27,32]. This process has been described previously [26] and consists of hydrogenase expression and activation using cell extract containing the three hydrogenase maturation genes necessary for activation [33,34], HydE, HydF, and HydG, from *S. oneidensis*. The maturases are anaerobically expressed in *E. coli* before lysis, and additional small-molecule substrates [35] are added to the cell-free reactions [26,27]. The epMotion 5070 liquid handler (Eppendorf North America, Westbury, NY) was used to increase the throughput of this process as described previously [27].

Cell-free protein synthesis was also used to produce the CpI mutants created by site-directed mutagenesis or saturation mutagenesis (Section 2.6). These cell-free protein synthesis reactions were performed in triplicate.

2.4. Methyl viologen hydrogenase activity assay

Hydrogenase activity was measured by monitoring methyl viologen reduction. CpI samples, either purified or in the cell-free reaction mixture, were added to 200 μL of 2 mM oxidized methyl viologen in 50 mM Tris pH 8 buffer, and the absorbance at 578 nm was monitored in a 96-well plate spectrophotometer. The amount of hydrogenase added to each well was adjusted to give a linear slope of A_{578} over the first 3 min. This slope and an extinction coefficient of 9.78 AU mM^{-1} cm^{-1} were used to calculate the methyl viologen reduction rate. The hydrogen consumption rate is then one-half of this value. This assay was performed anaerobically at room temperature in a glove box (Coy Laboratories, Grass Lake, MI) containing ~2% hydrogen and the balance nitrogen.

2.5. Oxygen exposure with air-saturated buffer addition

The *in vitro*-produced mutant CpI proteins were exposed to oxygen in the glove box by addition of air-saturated buffer [27]. The initial oxygen concentration was adjusted by modifying the amount of air-saturated buffer added, and a value was chosen that inactivated the wild-type protein to ~1–20% of the initial activity. After addition of the aerobic buffer, oxygen was allowed to diffuse out of the reaction solution into the glove box atmosphere and was most likely also consumed by the cell extract before the residual activity of the hydrogenase was measured. Care was taken to ensure that oxygen did not escape from the air-saturated Tris buffer prior to its addition to the diluted hydrogenase sample. A large bottle of air-saturated buffer was maintained outside the glove box, and the buffer transfer container was kept tightly sealed in the glove box until use.

For determination of oxygen sensitivity, the cell-free protein synthesis product was first diluted in anaerobic Tris buffer. A fraction of this diluted sample was removed and assayed for activity using the methyl viologen activity assay described above. This provided a value for the pre-O_2 exposure activity. The remaining protein was then exposed to oxygen. After 20 min, the resultant solution was assayed for residual hydrogenase activity, giving a value for the post-O_2 exposure activity. The ratio of the post-O_2 exposure activity to the pre-O_2 exposure activity was used to indicate oxygen sensitivity. This value was then compared to that of the wild-type protein to identify mutants with decreased oxygen sensitivity compared to the wild-type CpI. This same oxygen exposure method by air-saturated buffer addition was also used to evaluate purified CpI mutants.

2.6. In vivo CpI production and purification

CpI was produced using the [FeFe] hydrogenase production system developed by Kuchenreuther et al. [28] for producing high yields of active hydrogenase from *E. coli*. This process used the BL21(DE3) Δ*iscR* strain containing the pET-21(b)CpI plasmid and the pACYCDuet-1-*hydGX-hydEF* plasmid for CpI and maturase expression, respectively. An aerobic growth phase followed by anaerobic growth and expression was used for 50 mL cultures of each wild-type or mutant CpI. These cultures were lysed and the hydrogenase was anaerobically purified using 1 mL columns of *Strep*-Tactin® Superflow® high capacity resin (IBA GmbH, Germany) for each culture, as described [28].

2.7. Oxygen exposure of purified protein

To obtain a time course of oxygen inactivation for the mutant and wild-type enzymes, the purified protein was injected into 500 μL of 50 mM Tris buffer pH 8.0 in sealed 8 mL glass vials containing known amounts of oxygen in the headspace. The oxygen partial pressure was set by the volume of air injected into the headspace of each vial. The wild-type protein and mutant protein CpI N160D I197V A280V N289D were added to separate vials to an equivalent concentration of active protein before oxygen exposure (~10 nM based on a methyl viologen reduction specific activity of 476 μmol H_2 min^{-1} mg^{-1} for CpI [28]). At each time point, an aliquot of the diluted hydrogenase

solution was removed from the vial with a syringe and the enzyme activity was measured with the methyl viologen reduction assay (Section 2.4). The fraction of protein activity remaining was calculated by dividing the activity at each time point by the initial activity.

2.8. Saturation mutagenesis and site-directed mutagenesis

The QuikChange™ Site-Directed Mutagenesis Kit (Stratagene) was used to perform site-directed mutagenesis. For saturation mutagenesis at a given site, the procedure was performed 19 times with each alternative amino acid introduced by a different primer, and the desired sequences were confirmed by sequencing.

For mutant hydrogenase production by cell-free protein synthesis, the site-directed mutagenesis procedure was performed on the CpI gene in the pK7sCpI plasmid, then amplified via PCR using primers that annealed to the pK7 plasmid upstream and downstream of the T7 promoter and terminator, respectively. The PCR products were used as the DNA templates in the cell-free protein synthesis reactions. For *in vivo* protein production and purification, site-directed mutagenesis was performed on the CpI gene in the pET-21(b)CpI plasmid. These plasmids were then transformed into the production strain described above (Section 2.6).

2.9. Oxygen exposure during hydrogen production from NADPH

To test the oxygen tolerance of CpI while the enzyme was catalyzing hydrogen production, a system developed by Smith et al. [36] to produce hydrogen from NADPH was used. This system transfers electrons from NADPH to *Synechocystis* ferredoxin (Fd) using *E. coli* ferredoxin-NADPH-reductase (FNR); the CpI hydrogenase then converts electrons delivered by the reduced ferredoxin and protons into H_2.

For these tests, 100 μL reactions containing 50 mM Tris buffer pH 7, 0.1% Tween 20, 0.1 μM CpI, 70 μM FNR, 40 μM Fd, and 5 mM NADPH (Sigma–Aldrich) were used, along with 3 mM glucose-6-phosphate (Sigma–Aldrich) and 5 units of yeast glucose-6-phosphate dehydrogenase (Sigma–Aldrich) to regenerate NADPH. CpI was purified as described in Section 2.6, and the Fd and FNR were produced and purified as described by Smith et al. [36]. All reagents except NADPH were added to 8 mL vials and sealed in an anaerobic glove box (Coy Laboratories, Grass Lake, MI) containing a ~2% hydrogen (remainder nitrogen) environment. The reaction vials were removed from the glove box and heated to 37 °C, and the gas headspace was purged with oxygen-free nitrogen. NADPH was then injected to initiate the hydrogen production reactions. Hydrogen concentration in the headspace of the vials was measured using gas chromatography with a Hewlett Packard 6890 gas chromatograph (Hewlett Packard) and a ShinCarbon ST 100/120 mesh column (Resteck).

The rate of hydrogen production, as indicated by the accumulation of H_2 in the headspace, was monitored before and after the addition of air into the headspace of the vial. This was performed for both the wild-type CpI and mutant CpI I197S. Oxygen was introduced by injecting 2.65 mL of air into the headspace of the vial after 4 min of hydrogen production, resulting in 5% oxygen in the gas phase. As a control, the same reaction was monitored with pure N_2 injected into the headspace of the vial instead of air. The reaction was performed twice for each condition and the hydrogen concentration at each point was averaged.

2.10. Molecular graphics imaging

Molecular graphics images and measurement of atomic distances in the protein structure were produced using the UCSF Chimera package from the Resource for Biocomputing, Visualization, and Informatics at the University of California, San Francisco.

3. Results

3.1. Library creation and screening, and identification of a mutant with decreased oxygen sensitivity compared to the wild-type enzyme

The cell-free protein synthesis platform developed by Stapleton and Swartz [27] was used to produce and screen a library of mutant enzymes of [FeFe] hydrogenase I from *C. pasteurianum* (CpI) for decreased oxygen sensitivity. Nucleotide analogs [29] were used to create a set of libraries of CpI hydrogenase by random mutagenesis. The concentration of nucleotide analogs was varied from 2 to 200 μM and the number of PCR cycles from 20 to 30. The fraction of genes producing active hydrogenase mutants in the resulting libraries ranged between 0 and 60%. The final library used for screening was created with 8 μM analogs and 25 PCR cycles, and only about 1% of the mutants from the amplified genes retained activity above background. The mutated genes were then isolated by dilution before amplification by single-molecule PCR [32]. These mutant hydrogenase genes, spatially isolated by well, were then transcribed, translated, and activated *in vitro* [26] with the spatial link between the mutant protein and DNA sequence maintained. Of the approximately 3000 mutant genes that were screened for activity, 20 mutants that retained activity and consisted of a single gene population were collected. The genes expressing active hydrogenases were sequenced to identify the mutations and to confirm the presence of a unique sequence.

Sequencing revealed an average of 9 amino acid mutations (ranging from 4 to 16) in each 574 amino acid CpI protein, with 179 amino acid mutations in total. The mutations observed in the library are listed in Table 1. As shown, some amino acid mutations occurred with higher frequency than others. This bias matched well with that predicted for the dPTP and 8-oxo-dGTP mutagenesis method which heavily favors A to G and T to C transition mutations [29].

These 20 active hydrogenase mutants were then exposed to oxygen, and one mutant was identified with decreased oxygen sensitivity compared to the wild-type enzyme (Fig. 1B). This mutant also had significantly lower activity than the wild-type enzyme (Fig. 1A). There were 13 mutations in this M13 mutant: CpI S31P E47G R86H C153Y N160D D186G T188A I197V K208E K252R I253V A280V N289D, which are listed in Table 1.

Table 1 – Frequency of amino acid mutations identified in the 20 active mutant hydrogenases sequenced from the nucleotide analog mutagenesis library. The 13 mutations in M13 with decreased oxygen sensitivity and the influence of those mutations on activity and oxygen sensitivity is also listed.

Mutated from	Mutated to	Total in Library	In M13	Influence
Gly	Val	2		
Gly	Asp	3		
Ala	Val	5	A280V	↓ oxygen sensitivity
Ala	Thr	5		
Val	Ala	3		
Val	Ile	1		
Leu	Pro	4		
Leu	Gln	1		
Ile	Val	14	I197V, I253V	↓ oxygen sensitivity (197)
Ile	Leu	1		
Ile	Thr	7		
Met	Val	5		
Met	Thr	2		
Pro	Ser	1		
Phe	Val	1		
Phe	Leu	4		
Phe	Ser	4		
Phe	Thr	1		
Tyr	Cys	3		
Ser	Gly	1		
Ser	Pro	3	S31P	
Ser	Trp	2		
Thr	Ala	8	T188A	↓ activity
Thr	Ile	1		
Thr	Met	1		
Gln	Arg	4		
Asn	Tyr	1		
Asn	Ser	13		
Asn	His	1		
Asn	Asp	13	N160D, N289D	↓ oxygen sensitivity
Asn	Glu	1		
Cys	Tyr	2	C153Y	Fe-ligating cysteine
Cys	Arg	3		
Lys	Thr	2		
Lys	Arg	14	K252R	
Lys	Glu	14	K208E	
Arg	His	1	R86H	
Asp	Gly	7	D186G	↓ activity
Glu	Gly	13	E47G	
Glu	Lys	6		
Glu	Asp	1		
	Total Mutations:	179	13	

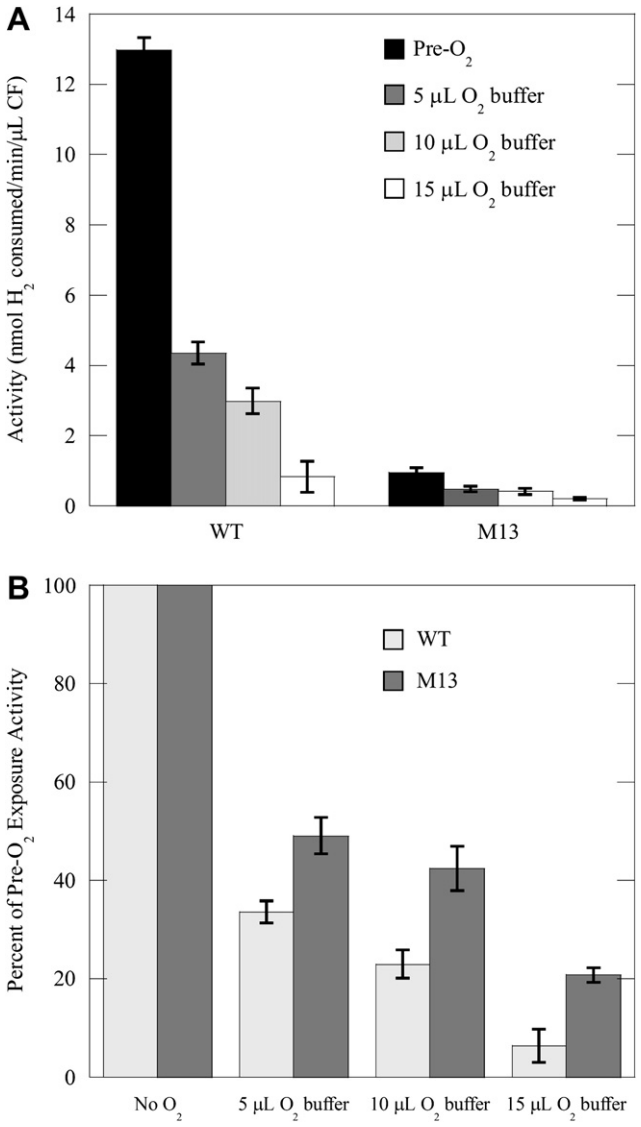

Fig. 1 – Oxygen inactivation of wild-type CpI and mutant M13. Cell-free reaction products (CF) were exposed to increasing oxygen concentrations by increasing the volume of air-saturated buffer added. (A) Hydrogen consumption activity before and after oxygen exposure, calculated from methyl viologen reduction rates. (B) Fraction of hydrogenase activity remaining after oxygen exposure. Error bars indicate the standard deviation of 3 independent assays.

3.2. *Identification of mutations responsible for decreased oxygen sensitivity*

Upon inspection of the crystal structure of CpI [9], it was noted that the mutation at amino acid 153 removed a ligating cysteine for an accessory [4Fe4S] cluster. Thinking that this mutation might be responsible for the loss of protein activity, the tyrosine mutation was restored to the wild-type cysteine. The activity of the resultant mutant, M12, was not restored, but the decreased oxygen sensitivity was retained.

Site-directed mutagenesis was then performed on M12 to individually restore each of the 12 mutations to the wild-type amino acid with the hope of identifying which of the 12 sites were influential for activity reduction and oxygen sensitivity. Restoration of position 186 from glycine to aspartic acid and position 188 from alanine to threonine was performed simultaneously (creating mutant M10) due to the close proximity of these two mutations on the gene. Restoration of positions 252 and 253 was also performed simultaneously,

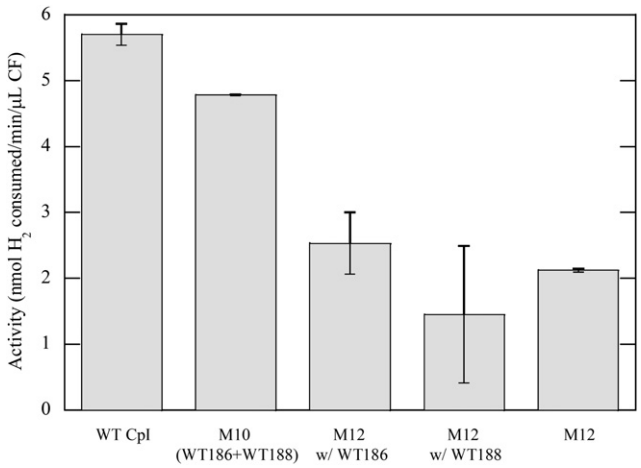

Fig. 2 – Restoration of activity to mutant M12. Hydrogen consumption activity of cell-free reaction products (CF) was measured for wild-type CpI, M12 mutant, and M12 mutant with only site 186, only 188, or both 186 and 188 (M10) restored to the wild-type amino acid. Hydrogen consumption activity was measured by methyl viologen reduction. Error bars indicate the standard deviation of 3 independent assays.

while the other 8 mutations were restored individually. Fortuitously, simultaneous restoration of both 186D and 188T restored activity to the protein (Fig. 2) while retaining the decreased oxygen sensitivity. Later investigations revealed that either mutation individually decreased the activity of the cell-free produced protein (Fig. 2).

The oxygen sensitivities of the cell-free produced M12 reversion mutants described above were also tested. The decreased oxygen sensitivity in M12 was lost when the asparagine at 289 was restored to the wild-type aspartic acid. Due to this initial result, N289D was assumed to be beneficial for decreased oxygen sensitivity.

Mutations were then introduced individually into the wild-type protein. Assuming that N289D was influential for oxygen sensitivity, this mutation was first introduced. However, CpI N289D showed the same oxygen sensitivity as the wild-type protein (data not shown). Assuming that a combination of mutations was responsible for the observed improvement, a second mutation from the set of 10 mutations in M10 was introduced into CpI N289D. Only one double mutant, CpI N289D I197V, showed any improvement over the wild-type enzyme, but this mutant still retained less activity after oxygen exposure than the M10 mutant (Fig. 3). Introducing N160D to CpI I197V N289D (Fig. 3) further improved the mutant, as did introducing A280V instead of N160D, but to a lesser extent (data not shown). Finally, introducing a fourth mutation to produce CpI N160D I197V A280V N289D (M4) improved the mutant activity after oxygen exposure even beyond that of the original M10 (Fig. 3). Addition of each of the remaining 6 mutations in M10 to M4 failed to further decrease oxygen sensitivity (data not shown).

The contributions of these 4 mutations were next investigated by oxygen exposure of purified proteins. The mutants were anaerobically expressed and activated *in vivo* in *E. coli*, and the enzymes were anaerobically purified as previously described [28]. It was observed that while the *in vivo* production of CpI I197V was comparable to wild-type CpI, adding additional mutations to CpI I197V decreased the amount of active hydrogenase in the cell lysate. It is not yet known whether decreased protein accumulation or incomplete activation was responsible for the lower active hydrogenase yields. After purification, the mutants were again assayed for oxygen sensitivity by addition of air-saturated buffer in the anaerobic chamber, and the activities before and after oxygen exposure were determined by measuring methyl viologen reduction. Confirming the results obtained with the cell-free reaction products, I197V alone decreased oxygen sensitivity,

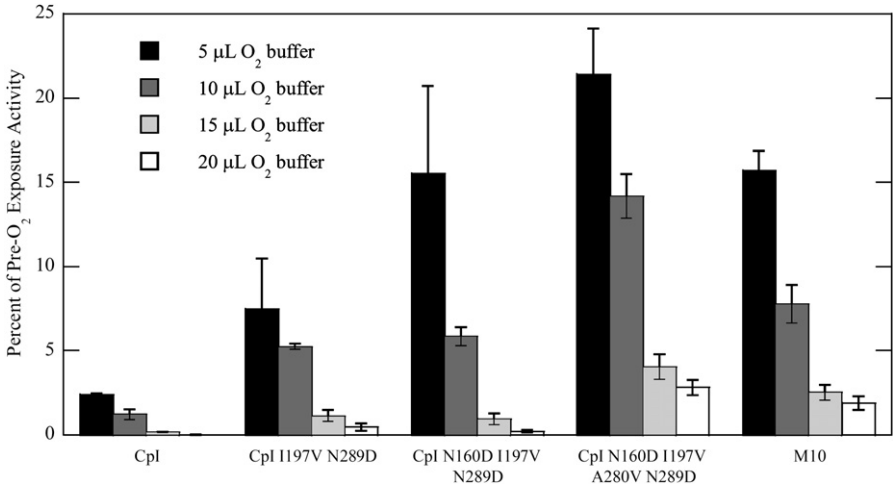

Fig. 3 – Mutations responsible for decreased oxygen sensitivity. The fraction of activity remaining after oxygen exposure was measured for cell-free reaction products of wild-type CpI, M10, and double, triple, or quadruple mutants of CpI N160D I197V A280V N289D. The oxygen exposure concentration was varied by increasing the volume of air-saturated buffer added. Methyl viologen reduction rate was used to calculate hydrogen consumption activity before and after oxygen exposure. Error bars indicate the standard deviation of 3 independent assays.

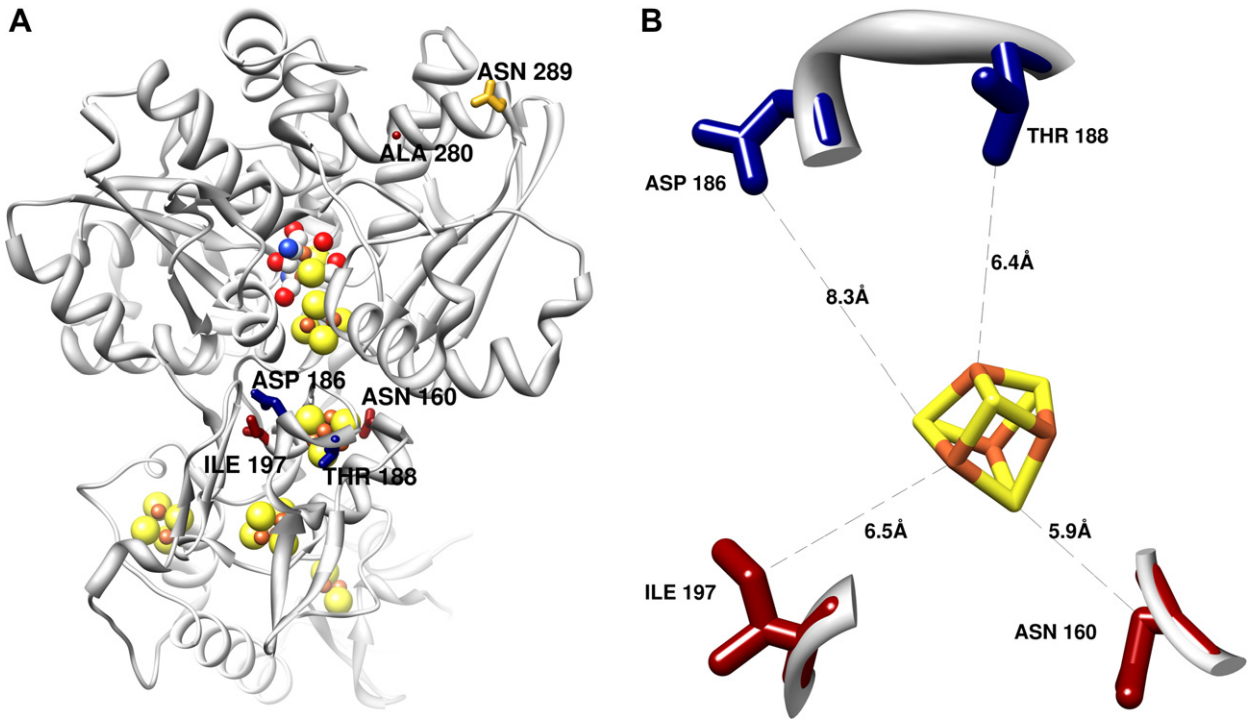

Fig. 4 – (A) Structure of CpI indicating the locations of positions 160, 197, and 280 influential for oxygen sensitivity (red), positions 186 and 188 influential for activity (blue), and position 289 influential for oxygen sensitivity in M12 (orange). (B) The accessory [4Fe4S] cluster proximal to the H-cluster in CpI is shown with nearby positions influential for activity (blue) and oxygen sensitivity (red).

and N160D and A280V further improved the enzyme (Fig. 5). However, N289D had no effect on the oxygen sensitivity of the purified mutants tested (Fig. 5). It is possible that the initial effect observed previously from N289D was dependent upon interactions with amino acid changes no longer present in these mutants.

The locations of the three influential mutations (160, 197, and 280), the potentially influential mutation (289), and the two mutations affecting activity (186 and 188), are shown in Fig. 4. The side chains of amino acids 160, 197, 186 and 188 are within 5.9 Å, 6.5 Å, 8.3 Å, and 6.4 Å, respectively, of the accessory [4Fe4S] cluster proximal to the H-cluster in the wild-type CpI crystal structure [9]. Amino acid 280 has been identified as an amino acid lining one of the predicted oxygen diffusion channels [37]. Amino acid 289 is not located in a channel or near an [FeS] cluster but instead is near the surface of the protein.

3.3. *Oxygen sensitivity as indicated by methyl viologen reduction activity*

The oxygen sensitivities of the wild-type and mutant proteins was additionally compared by exposing both proteins to 1% O_2 in the gas phase and monitoring hydrogenase inactivation over time as indicated by residual methyl viologen reduction activity. Oxygen inactivation curves of wild-type CpI and M4 mutant CpI N160D I197V A280V N289D are shown in Fig. 6. The mutant retained significantly more activity than the wild-type enzyme: the M4 hydrogenase retained 62% activity 5 min into the oxygen exposure while only 23% of the wild-type activity remained. After 12.5 min, the mutant was still 22% active while the wild-type protein only retained 8% activity. While the wild-type hydrogenase was inactivated more rapidly than the mutant, both proteins were almost completely inactive after ~30 min in 1% O_2.

3.4. *Saturation mutagenesis at influential sites further decreases oxygen sensitivity*

To search for further improved mutants, saturation mutagenesis was performed at each of the 4 sites originally identified as influential for oxygen sensitivity: 160, 197, 280, and 289. The activity and oxygen sensitivity of the 19 mutants created with site-directed mutagenesis at each site were compared using the same sequence of protein production and activation via cell-free protein synthesis, oxygen exposure via air-saturated buffer addition, and pre-O_2 and post-O_2 activity measurements using hydrogen consumption and methyl viologen reduction.

Saturation mutagenesis at site 289 was performed on the M4 mutant CpI N160D I197V A280V N289D. No amino acid substitutions at this site affected oxygen sensitivity when the other 3 mutations were present (Supplemental Fig. 1). As also observed at the other 3 sites, some amino acid substitutions (for example, proline) were deleterious to activity.

Saturation mutagenesis at site 197 was conducted on both the wild-type CpI and the M4 mutant. Several single and

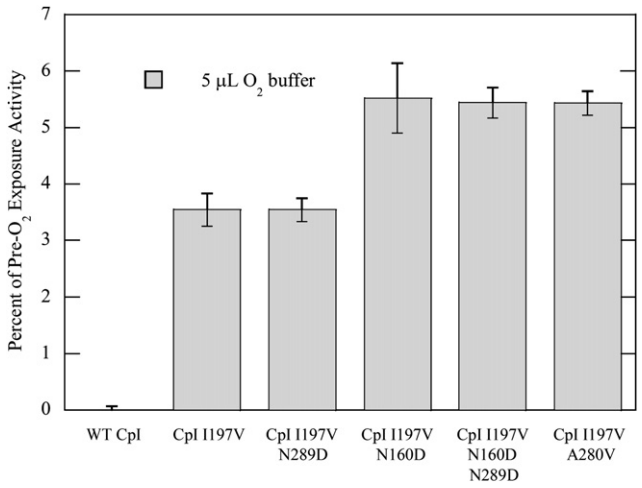

Fig. 5 – Influence of sites 160, 197, 280, and 289 on oxygen sensitivity, as indicated by the fraction of methyl viologen reduction activity remaining after oxygen exposure of purified protein. Error bars indicate the standard deviation of 3 independent assays.

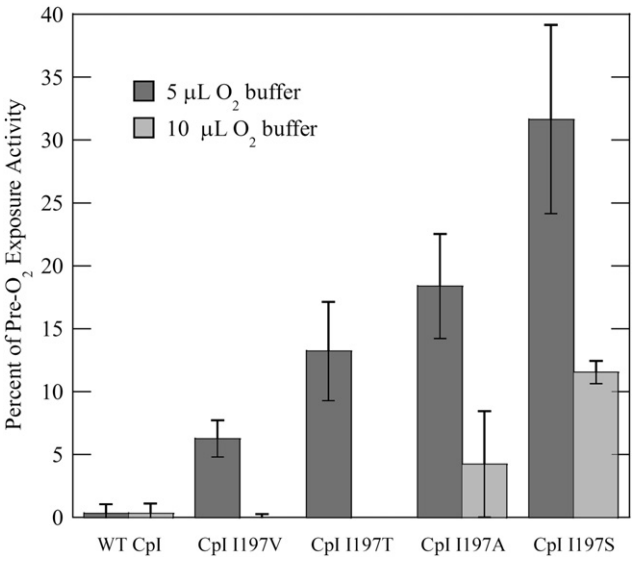

Fig. 7 – Decreased oxygen sensitivity by mutation of position 197, as indicated by the fraction of methyl viologen reduction activity remaining after oxygen exposure of purified protein. Error bars indicate the standard deviation of 3 independent assays.

quadruple mutant proteins showed higher residual activity after oxygen exposure than either the wild-type protein (isoleucine at 197) or the originally isolated valine mutant (single mutation results shown in Supplemental Fig. 2). Four promising single 197 mutants were purified and tested for oxygen sensitivity. Serine conferred the greatest decrease in oxygen sensitivity, followed by alanine, threonine, and valine, respectively (Fig. 7). A new quadruple mutant with I197S, CpI N160D I197S A280V N289D (M4S), was used as the template for the next two rounds of saturation mutagenesis because it was the least sensitive mutant observed up to this point.

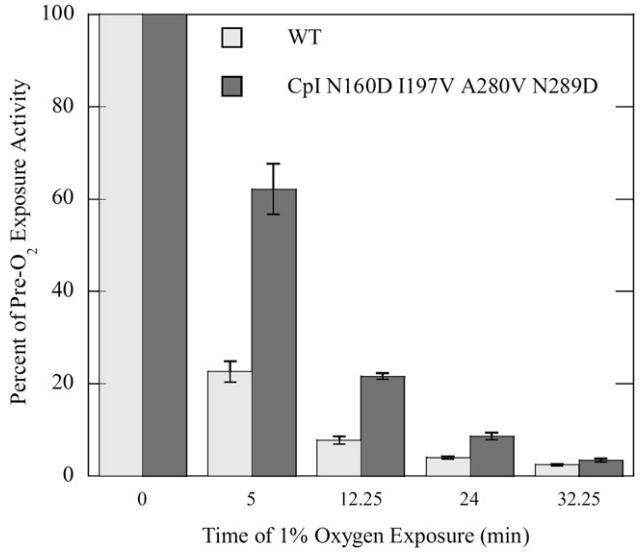

Fig. 6 – Decreased oxygen sensitivity of M4. Purified protein was exposed to 1% oxygen in the headspace of a sealed vial and sampled after various exposure times. The fraction of hydrogen consumption activity remaining at each time point was calculated from the methyl viologen reduction rate. Error bars indicate the standard deviation of 3 independent assays.

Saturation mutagenesis at site 280 revealed that the originally identified mutation, alanine to valine, provided the best improvement at that site (Supplemental Fig. 3). Most of the other 18 amino acids made the hydrogenase more sensitive to oxygen inactivation than the protein with the wild-type alanine 280. The site does appear to be influential for oxygen sensitivity when N160D I197S and N289D are present, and in this background the originally identified A280V is the only mutation that provides an improvement.

In saturation mutagenesis experiments on the M4S mutant, site 160 did not appear to be influential. The wild-type asparagine, the originally identified mutant aspartic acid, and most other permissible mutations resulted in equivalent oxygen inactivation. Therefore, while this site had been influential when valine was present at position 197 (Fig. 5), it does not seem to be influential with I197S (Supplemental Fig. 4). The mutant with the lowest oxygen sensitivity without non-influential mutations is therefore CpI I197S A280V. However, because the *in vivo* accumulation of active CpI I197S A280V was significantly lower than that of CpI I197S, and since I197S provided the most significant contribution to decreased oxygen sensitivity, the CpI I197S mutant was chosen for characterization of oxygen sensitivity during hydrogen production.

3.5. *Oxygen exposure during hydrogen production from reduced ferredoxin*

In order to characterize the oxygen tolerance of the wild-type CpI and CpI I197S while actively producing hydrogen, a system developed by Smith et al. [36] to produce hydrogen from NADPH was used. This system directs electron transfer from NADPH through ferredoxin-NADPH-reductase (FNR) and

ferredoxin to CpI and can be used to measure hydrogen production from CpI with or without oxygen present in the headspace of the vial.

To ensure that the hydrogen production rate was representative of active CpI concentration (and the reaction was not rate-limited by another step in electron transfer from NADPH to CpI), low CpI concentrations were used. With 0.1 μM hydrogenase, the hydrogenase activity limited the hydrogen production rate (data not shown). Upon oxygen addition, it is possible that part of the decrease in the hydrogen production rate was due to oxidation of ferredoxin rather than inactivation of CpI, but any inefficiency in electron transfer due to ferredoxin oxidation should be equivalent between the mutant and wild-type reaction vials. An additional control showed no hydrogen production in the absence of hydrogenase, as expected.

For these reactions, oxygen was introduced after 4 min of hydrogen production by injecting air into the headspace of the vial, resulting in 5% oxygen in the gas phase. The hydrogen production rates for CpI and CpI I197S with and without oxygen exposure are shown in Fig. 8. While the rate of hydrogen production decreased slightly over the course of the reaction even in the absence of oxygen, likely due to thermodynamic limitations, the decline in production rate was much more pronounced after oxygen addition. Even after 25 min of 5% oxygen exposure, there is some residual activity of the hydrogenases. As shown, however, the mutant and wild-type enzyme appeared to be equally sensitive to oxygen inactivation. Lower oxygen concentrations in the headspace also showed that CpI I197S inactivated at a similar rate to wild-type CpI (data not shown). This equivalent inactivation rate suggests that the mutant provides no improvement in oxygen tolerance over the wild-type enzyme when the hydrogenase is actively producing hydrogen at the time of oxygen exposure.

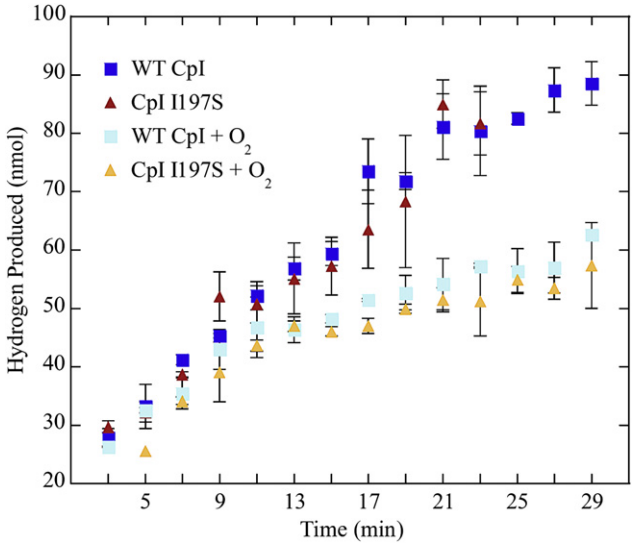

Fig. 8 – Oxygen inactivation of purified hydrogenases CpI and CpI I197S when actively producing hydrogen from reduced ferredoxin using the NADPH to H_2 production system. The hydrogen concentration at each time point was measured, and 5% oxygen was introduced into the headspace of the vial at 4 min. Error bars indicate the standard deviation of 2 independent assays.

4. Discussion

4.1. *Identification of a mutant with decreased oxygen sensitivity compared to the wild-type CpI*

Dynamic modeling of the 3-D structure of the [FeFe] hydrogenase CpI suggests two main channels for oxygen diffusion to the active site, where oxygen can then bind and destroy the H-cluster, killing enzyme activity [37]. One suggested approach for producing an oxygen-tolerant [FeFe] hydrogenase is to modify the protein structure so that oxygen access to the active site is physically restricted, protecting the active site from attack. This limited access of oxygen to the active site is believed to be the mechanism of oxygen tolerance for some [NiFe] hydrogenases that catalyze the hydrogen consumption reaction [24]. However, despite rational engineering attempts to constrict the two predicted oxygen diffusion channels, no mutants with significantly improved oxygen tolerance have been identified [38].

Because all of the oxygen diffusion channels to the active site may not be known and/or rational protein design may not accurately predict the mutations required to improve oxygen tolerance, a random mutagenesis and screening method was chosen for this directed evolution project. The platform used here for producing [26] and screening a library of mutant [FeFe] hydrogenases was previously developed for the [FeFe] hydrogenase HydA1 from *Chlamydomonas reinhardtii*. In that study, none of the ~30,000 HydA1 mutants screened were found to have improved oxygen tolerance [27]. For this screen, CpI from *C. pasteurianum* was chosen. CpI has a faster hydrogen production rate than HydA1 [28], has a longer half-life in air than HydA1 [25], and it appears from the 3-D structures that the CpI active site is more protected by the surrounding protein structure than the more open HydA1 active site [9,39].

For this library, random mutagenesis of CpI was performed to introduce multiple mutations per gene. Fewer than 1% of the mutant library retained significant activity, and the sequenced active mutants had an average of 9 amino acid mutations per protein. This high mutation rate was chosen because of the possibility that no significant improvement in oxygen tolerance could be achieved without simultaneous mutations at multiple sites within the protein. For example, both oxygen diffusion channels might have required diffusional restrictions. This mutagenesis strategy is contrary to the usual approach, in which a low mutation rate maintains a high fraction of active mutants and allows improvements in the characteristic of interest to be incrementally evolved. In this screen, because activity both before and after oxygen exposure was measured, decreased oxygen sensitivity could be identified even when mutants also contained mutations detrimental to protein activity.

The advantage of using a high mutational load was demonstrated by the discovery of a mutant of interest among the first 20 active mutants screened, despite the significantly lower activity of that protein relative to the wild-type protein

(Fig. 1). Individual reversion of the 13 mutations in this M13 mutant was then used to restore activity (Fig. 2), and individual introduction of these mutations was used to identify the three mutations responsible for the decreased oxygen sensitivity: N160D, I197V, and A280V (Fig. 3). Neither N160D nor A280V provided any advantage individually and would not have been identified had they been tested in a low mutation rate library. However, the combination of I197V, N160D, and A280V cooperatively decreased the oxygen sensitivity to a level where the mutant could be identified relative to the background variance of the screen. It was most likely very fortuitous that this mutant, with three cooperative mutations, was identified so early in the screen, with only 159 unique amino acid mutations occurring in the library of 20 active mutants.

It was also fortuitous that the beneficial mutations were favored by the bias of the mutagenesis method using nucleotide analogs, shown in Table 1. The most frequent base transition mutation, A to G, was responsible for creating the amino acid mutations N160D and I197V, and the less frequent but still present C to T transition mutation was responsible for creating the A280V amino acid mutation. Continued screening may or may not have identified further mutants of interest with decreased oxygen sensitivity, but screening was stopped to better characterize and understand the mutations responsible for the improvement in the M13 mutant. Beneficial mutations were then intended to be used in the starting template for a second round of mutagenesis.

4.2. *Mutations responsible for decreased activity and decreased oxygen sensitivity in CpI*

The location of the two amino acid mutations, D186G and T188A, responsible for the decrease in activity of the originally identified mutant M13 (Fig. 2) are shown in Fig. 4. These amino acids, D186 and T188, are within 8.3 and 6.4 Å, respectively, of the accessory [4Fe4S] cluster proximal to the active site. Given their locations, it is likely that these mutations are influencing electron transfer through this proximal FeS cluster, either by changing the cluster itself or by changing the ability of methyl viologen to access the [FeS] cluster. The exact pathway of electron transfer from the H-cluster to methyl viologen in CpI has not been determined, but the influence of these two mutations suggests that this accessory FeS cluster is involved in the process. These mutations were restored without affecting the decreased oxygen sensitivity.

The location of the three mutations responsible for cooperatively decreasing the oxygen sensitivity of CpI, amino acids 160, 197, and 280, are also shown in Fig. 4. Position 280 is located in one of the two predicted oxygen diffusion channels [37]. Instead of replacing a small amino acid with a large bulky or hydrophobic amino acid as was predicted to be necessary to restrict oxygen diffusion in the channel [25], however, the identified change was fairly conservative. The only mutation at this site that improved the enzyme with N160D I197V N289D also present was the originally identified alanine to valine mutation. Although valine is slightly larger than alanine, most other substitutions, including the introduction of bulky hydrophobic amino acids, actually increased the oxygen sensitivity (Supplementary Fig. 3B) instead of making the enzyme less sensitive to oxygen inactivation. This mutation alone did not influence the oxygen sensitivity, but was influential when the change at 197 was also present.

The most influential position was 197, as I197V was the only individual mutation that measurably decreased oxygen sensitivity. N160D and A280V both further decreased oxygen sensitivity (Fig. 3), but only if I197V was also present (data not shown). Saturation mutagenesis at site 197 then identified mutants that were significantly improved over the original I197V mutation (Fig. 7). The amino acids that decreased oxygen sensitivity were all uncharged residues smaller than the wild-type isoleucine. Serine provided the greatest improvement of the mutants purified, with alanine, threonine, and valine also decreasing the oxygen sensitivity relative to the wild-type isoleucine (Fig. 7).

Sites 160 and 197 are both located near the proximal accessory [4Fe4S] cluster of CpI. This location in the protein is not one that would have been predicted as influential for limiting oxygen diffusion to the active site [37]. These amino acid mutations may indeed be restricting oxygen diffusion, either through long-range protein structural changes constricting the predicted oxygen diffusion channels or by constricting a channel near these two sites that had not been previously predicted. However, as both mutations are located within 6.5 Å of the first accessory [4Fe4S] cluster of CpI (Fig. 4b), it is likely that the changes are instead affecting that [FeS] cluster. These changes may be limiting oxygen access to the [4Fe4S] cluster or may be changing the oxygen reactivity of the cluster, for example. It is possible that the decreased oxygen sensitivity is due to an altered redox potential of this proximal accessory [FeS] cluster. It is interesting to note that one mechanism of oxygen tolerance in [NiFe] hydrogenases appears to be a high redox potential of the proximal accessory [4Fe4S] cluster [22]. The data in Fig. 7 suggest that small side chain volume and the presence of a hydroxyl group are beneficial for decreased oxygen sensitivity at position 197. In the former case, the small side chain may be influencing the [FeS] center geometry. In the latter case, the hydroxyl group may be serving as a hydrogen bond donor to change the electrostatic character of the protein environment surrounding the [FeS] center. Additionally, if 160 and 197 are in fact both influencing the redox potential of the [FeS] cluster, it is perhaps not surprising that site 160 is no longer influential when combined with the significantly improved I197S mutant rather than the original I197V mutant.

The location of amino acid 289 is also shown in Fig. 4A. The 289 site was influential for oxygen sensitivity in the originally identified mutant M12 with 12 mutations and also in the mutant M10 with 10 mutations and activity restored. Restoring the aspartic acid at amino acid 289 to the wild-type asparagine increased the oxygen sensitivity of both of these proteins back to that of the wild-type. However, when N289D was introduced into the wild-type protein alone or when saturation mutagenesis was performed at that site with CpI N160D I197V A280V, the position did not influence oxygen sensitivity. One possible explanation for the conflicting data on the influence of this location is that one or more of the other 6 mutations in M10 could provide an influence that is cooperative with N289D. It remains unclear why reverting the I197V mutation in M12 failed to influence oxygen sensitivity.

4.3. *Characterization of the oxygen sensitivity of the mutant and wild-type CpI*

When the hydrogenase is not actively catalyzing a reaction during oxygen exposure, and the activity before and after oxygen exposure is measured by the rate of methyl viologen reduction, the mutant hydrogenase is significantly more stable against oxygen inactivation than the wild-type enzyme. For example, after a 5 min oxygen exposure to 1% O_2, the wild-type protein retained only 23% of its initial activity, while the mutant CpI N160D I197V A280V N289D retained 62% (Fig. 6).

However, when the oxygen exposure is performed while the enzyme is actively producing hydrogen from reduced ferredoxin, the mutant does not show improved oxygen tolerance. CpI I197S appears to be equally inactivated relative to the wild-type enzyme in a 5% oxygen atmosphere (Fig. 8). This enzyme, therefore, does not appear to be more oxygen-tolerant during catalysis, but only more resistant to oxygen inactivation while in a resting state, as indicated by residual methyl viologen reduction activity after oxygen exposure. This dependence of measured oxygen sensitivity on the exposure conditions, along with the proximity of the most influential mutation to the proximal accessory [FeS] cluster, illustrates the complexity of the oxygen inactivation process of CpI.

The effect of the [FeFe] hydrogenase redox state during oxygen exposure has previously been investigated by Goldet et al. using protein film electrochemistry [16]. They found that the [FeFe] hydrogenases from *Desulfovibrio desulfuricans* and *Clostridium acetobutylicum* were more rapidly inactivated when exposed to oxygen during hydrogen oxidation than during hydrogen production. The [FeFe] hydrogenase from *C. reinhardtii*, however, had comparable inactivation rates under reducing or oxidizing potentials. While the *C. pasteurianum* CpI enzyme was not tested in this study, this observed difference in oxygen sensitivity during hydrogen production and consumption may offer an explanation for the discrepancy between the CpI and CpI I197S sensitivities with the different oxygen exposure assays.

Oxygen tolerance during hydrogen production from reduced ferredoxin, compared to tolerance in the hydrogen consumption direction with methyl viologen as an artificial electron acceptor, more accurately mimics the *in vivo* application of an oxygen-tolerant hydrogenase in a photosynthetic organism. Thus the mutant hydrogenase identified in this screen does not appear immediately useful for *in vivo* applications. A screen is therefore needed that measures oxygen tolerance while the proteins are actively catalyzing hydrogen production. The cell-free production and screening method described here for CpI is currently being modified to do so. The mutations identified in this study may still prove beneficial and are the subject of ongoing investigations.

5. Conclusion

High frequency mutagenesis coupled with a cell-free screen appears to be effective for identifying hydrogenases with altered phenotypes. However, it is now apparent that the screen must test for the precise phenotype that is desired. In this study, hydrogen consumption activity was used to identify a mutant less sensitive to oxygen exposure while in a resting state. However, the mutant was just as sensitive to oxygen as the wild-type hydrogenase when actively producing hydrogen. This observation, along with the proximity of the influential mutations to the accessory [FeS] cluster, demonstrates the complexity of the oxygen inactivation of CpI, which may involve the accessory [FeS] clusters as well as gas diffusion channels and the active site. The mutant identified here is likely not immediately useful for hydrogen production applications, and the screen for an oxygen-tolerant hydrogenase is currently being modified to identify mutants with improved hydrogen production capabilities in the presence of oxygen.

Acknowledgments

The authors thank Kunal Mehta and Rachel Bent for their work on the saturation mutagenesis experiments, and Monica Ortiz for her work on the library screen. This work was supported by the Global Climate and Energy Project (GCEP) at Stanford University (SPO # 35293 and SPO # 44473) and by the DOE Office of Basic Energy Sciences (DE-FG02-09ER46632). The UCSF Chimera package from the Resource for Biocomputing, Visualization, and Informatics at the University of California, San Francisco was supported by NIH grant P41 RR-01081.

Appendix. Supplementary material

Supplementary data related to this article can be found online at doi:10.1016/j.ijhydene.2011.02.048.

REFERENCES

[1] Das D, Veziroglu T. Advances in biological hydrogen production processes. Int J Hydrogen Energy 2008;33:6046–57.
[2] Dasgupta C, Gilbert J, Lindblad P, Heidorn T, Borgvang S, Skjanes K, et al. Recent trends on the development of photobiological processes and photobioreactors for the improvement of hydrogen production. Int J Hydrogen Energy 2010;35:10218–38.
[3] Hallenbeck P, Benemann J. Biological hydrogen production; fundamentals and limiting processes. Int J Hydrogen Energy 2002;27:1185–93.
[4] Ghirardi M, Posewitz M, Maness P, Dubini A, Yu J, Seibert M. Hydrogenases and hydrogen photoproduction in oxygenic photosynthetic organisms. Plant Biol 2007;58:71.
[5] Vignais P, Billoud B. Occurrence, classification, and biological function of hydrogenases: an overview. Chem Rev 2007;107:4206–72.
[6] Frey M. Hydrogenases: hydrogen-activating enzymes. ChemBioChem 2002;3:153–60.
[7] Peters J. Structure and mechanism of iron-only hydrogenases. Curr Opin Struct Biol 1999;9:670–6.
[8] Nicolet Y, Cavazza C, Fontecilla-Camps J. Fe-only hydrogenases: structure, function and evolution. J Inorg Biochem 2002;91:1–8.
[9] Peters J, Lanzilotta W, Lemon B, Seefeldt L. X-ray crystal structure of the Fe-only hydrogenase (CpI) from *Clostridium*

pasteurianum to 1.8 angstrom resolution. Science 1998;282:1853.
[10] Stripp S, Goldet G, Brandmayr C, Sanganas O, Vincent K, Haumann M, et al. How oxygen attacks [FeFe] hydrogenases from photosynthetic organisms. Proc Natl Acad Sci USA 2009;106:17331.
[11] Lemon B, Peters J. Binding of exogenously added carbon monoxide at the active site of the iron-only hydrogenase (CpI) from *Clostridium pasteurianum*. Biochemistry 1999;38:12969–73.
[12] De Lacey A, Fernandez V, Rousset M, Cammack R. Activation and inactivation of hydrogenase function and the catalytic cycle: spectroelectrochemical studies. Chem Rev 2007;107:4304–30.
[13] Vincent K, Parkin A, Armstrong F. Investigating and exploiting the electrocatalytic properties of hydrogenases. Chem Rev 2007;107:4366–413.
[14] Liebgott P, Leroux F, Burlat B, Dementin S, Baffert C, Lautier T, et al. Relating diffusion along the substrate tunnel and oxygen sensitivity in hydrogenase. Nat Chem Biol 2010;6:63–70.
[15] Vincent K, Parkin A, Lenz O, Albracht S, Fontecilla-Camps J, Cammack R, et al. Electrochemical definitions of O_2 sensitivity and oxidative inactivation in hydrogenases. J Am Chem Soc 2005;127:18179–89.
[16] Goldet G, Brandmayr C, Stripp S, Happe T, Cavazza C, Fontecilla-Camps J, et al. Electrochemical kinetic investigations of the reactions of [FeFe]-hydrogenases with carbon monoxide and oxygen: comparing the importance of gas tunnels and active-site electronic/redox effects. J Am Chem Soc 2009;131:14979–89.
[17] Singh B, Curdt I, Shomburg D, Bisen P, Bhöme H. Valine 77 of heterocystous ferredoxin FdxH2 in Anabaena variabilis strain ATCC 29413 is critical for its oxygen sensitivity. Mol Cell Biochem 2001;217:137–42.
[18] Fontecilla-Camps J, Volbeda A, Cavazza C, Nicolet Y. Structure/function relationships of [NiFe]-and [FeFe]-hydrogenases. Chem Rev 2007;107:4273–303.
[19] Guiral M, Tron P, Belle V, Aubert C, Léger C, Guigliarelli B, et al. Hyperthermostable and oxygen resistant hydrogenases from a hyperthermophilic bacterium *Aquifex aeolicus*: physicochemical properties. Int J Hydrogen Energy 2006;31:1424–31.
[20] Infossi P, Lojou E, Chauvin J, Herbette G, Brugna M, Giudici-Orticoni M. *Aquifex aeolicus* membrane hydrogenase for hydrogen biooxidation: role of lipids and physiological partners in enzyme stability and activity. Int J Hydrogen Energy 2010;35:10778–89.
[21] Goldet G, Wait A, Cracknell J, Vincent K, Ludwig M, Lenz O, et al. Hydrogen production under aerobic conditions by membrane-bound hydrogenases from *Ralstonia* species. J Am Chem Soc 2008;130:11106–13.
[22] Lenz O, Ludwig M, Schubert T, Bürstel I, Ganskow S, Goris T, et al. H_2 conversion in the presence of O_2 as performed by the membrane bound [NiFe] hydrogenase of *Ralstonia eutropha*. ChemPhysChem 2010;11:1107–19.
[23] Saggu M, Zebger I, Ludwig M, Lenz O, Friedrich B, Hildebrandt P, et al. Spectroscopic insights into the oxygen-tolerant membrane-associated [NiFe] hydrogenase of *Ralstonia eutropha* H16. J Biol Chem 2009;284:16264.
[24] Buhrke T, Lenz O, Krauss N, Friedrich B. Oxygen tolerance of the H2-sensing [NiFe] hydrogenase from *Ralstonia eutropha* H16 is based on limited access of oxygen to the active site. J Biol Chem 2005;280:23791.
[25] Cohen J, Kim K, Posewitz M, Ghirardi M, Schulten K, Seibert M, et al. Molecular dynamics and experimental investigation of H_2 and O_2 diffusion in [Fe]-hydrogenase. Biochem Soc Trans 2005;33:80.
[26] Boyer ME, Stapleton JA, Kuchenreuther JM, Wang CW, Swartz JR. Cell free synthesis and maturation of [FeFe] hydrogenases. Biotechnol Bioeng 2008;99:59–67.
[27] Stapleton JA, Swartz JR. A cell-free microtiter plate screen for improved [FeFe] hydrogenases. PLoS One 2010;5:e10554.
[28] Kuchenreuther JM, Grady-Smith CS, Bingham AS, George SJ, Cramer SP, Swartz JR. High-yield expression of heterologous [FeFe] hydrogenases in *Escherichia coli*. PLoS One 2010;5:e15491.
[29] Zaccolo M, Williams DM, Brown DM, Gherardi E. An approach to random mutagenesis of DNA using mixtures of triphosphate derivatives of nucleoside analogues. J Mol Biol 1996;255:589–603.
[30] Koga Y, Kobayashi K, Yang J, Nakano H, Yamane T. In vitro construction and screening of a Burkholderia cepacia lipase library using single-molecule PCR and cell-free protein synthesis. J Biosci Bioeng 2002;94:84–6.
[31] Ohuchi S, Nakano H, Yamane T. In vitro method for the generation of protein libraries using PCR amplification of a single DNA molecule and coupled transcription/translation. Nucleic Acids Res 1998;26:4339.
[32] Rungpragayphan S, Yamane T, Nakano H. SIMPLEX: single-molecule PCR-linked in vitro expression: a novel method for high-throughput construction and screening of protein libraries. Methods Mol Biol 2007;375:79–94.
[33] Posewitz M, King P, Smolinski S, Zhang L, Seibert M, Ghirardi M. Discovery of two novel radical S-adenosylmethionine proteins required for the assembly of an active [Fe] hydrogenase. J Biol Chem 2004;279:25711.
[34] Nicolet Y, Fontecilla-Camps J, Fontecave M. Maturation of [FeFe]-hydrogenases: structures and mechanisms. Int J Hydrogen Energy 2010;35:10750–60.
[35] Kuchenreuther J, Stapleton J, Swartz J. Tyrosine, cysteine, and S-adenosyl methionine stimulate in vitro [FeFe] hydrogenase activation. PLoS One 2009;10:e7565.
[36] Smith PR, Bingham AS, Swartz JR. Generation of hydrogen from NADPH using an [FeFe] hydrogenase. Int J Hydrogen Energy 2012;37:2977–83.
[37] Cohen J, Kim K, King P, Seibert M, Schulten K. Finding gas diffusion pathways in proteins: application to O_2 and H_2 transport in CpI [FeFe]-hydrogenase and the role of packing defects. Structure 2005;13:1321–9.
[38] Ghirardi M, Cohen J, King P, Schulten K, Kim K, Seibert M. [FeFe]-hydrogenases and photobiological hydrogen production. Proc SPIE 2006;6340. 63400X.
[39] Mulder D, Boyd E, Sarma R, Lange R, Endrizzi J, Broderick J, et al. Stepwise [FeFe]-hydrogenase H-cluster assembly revealed in the structure of HydA EFG. Nature 2010;465:248–51.